Recognition of the Making on Integrated Circuit Chips Based On the Hybrid Fourier-AFMT

Yee Ming Chen[1] Jen-Hong Chiang[2]

***Abstract*-In this paper, an automatic optical inspection system incorporating optical character recognition (OCR) is employed to inspect markings on integrated circuit (IC) chips. Here, we present a novel OCR-based method for character recognition based on the features extracted from the integrated discrete wavelet and the hybrid Fourier-AFMT framework (DWF-AFMT) which is fast and yields better results as compared to basic Fourier Mellin Transform. We focus on the computation of a new set of invariant features allowing the classification of multi-oriented and multi-scaled patterns. Discrete Wavelet transform was used to smooth and preserve the local edges after image decomposition, making the character images less sensitive to shape distortion whilst Fourier-AFMT served to produce a translation, rotation and scale invariant feature, Multiple DWF-AFMT features could be used to form a reference invariant feature through the linearity property of Fourier-AFMT and reduce the variability of input images. The experiments showed the recognition rate reached over 100% when multiple DWF-AFMT features were used.**

Keywords-Printed marking recognition, analytical Fourier-Mellin transform (AFMT), Wavelet transforms, Optical Character Recognition (OCR)\

I. Introduction

Automatic optical inspection (AOI) system vision has many important applications in the electronics manufacturing industry, including the evaluation and testing of electronic components, inspection of IC chips. In a manufacturing system, the IC chips are lined up in a running conveyor for marking inspection. Markings on the IC chips are captured as a movie clip by a charged couple device (CCD) (Figure1). In machine vision inspecting markings on IC chips, an incorrect decision on marking may result in inappropriate placement of chip on printed circuit board during assembly process. The software then identifies whether the IC marking is of good quality. Thus automatic inspection of IC markings attracted considerable interest (Cho et al., 2005). The software, are used to convert characters in the images to their corresponding ASCII values for subsequent operations. However, poor lighting conditions during image capture can seriously degrade the quality of the digitized image; especially images captured in non-uniform illumination conditions are often noisy and low in contrast. Both these image acquisition methods degrade the quality of the digitized image, and directly influence the accuracy of character recognition

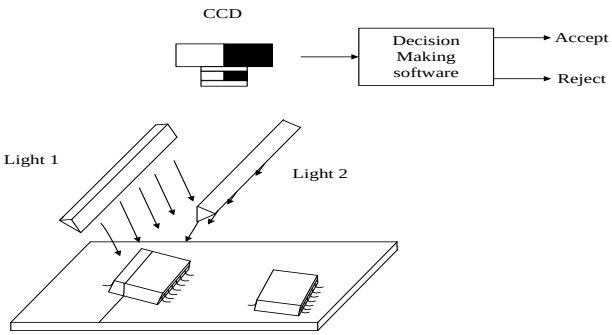

Figure 1. IC chip marking inspection system

The problem of finding reliable detection performance of the AOI for the character area for recognition of object IC chips marks is nowadays more present than ever. Since 1950, Optical Character Recognition (OCR) has been very active in the application of automatic pattern recognition, now it is used to read the printed characters at high speed (Mantas, 1986; Shunji et al, 1992). OCR is widely used in recognition of hand written characters and printed characters using Artificial Intelligence techniques (Mantas, 1986; Shunji et al, 1992; Adnan et al., 1996; Nagarajan et al., 2003). The OCR is applied for business card recognition (Wumo et al., 2001) where the manual input is optional, however, by scanning; the OCR is able to create an easier database. The document reading and analysis have reached an important position in certain markets. The application of OCR in the postal automation has followed into the banks and industrial recognition processes (Rafael and Richard, 1993; Mauritius and Christopher, 2001; Oivind et al., 1996). A popular technique to analyze images for the purpose of automatic recognition is supervised learning. In supervised learning a representative set of images is available from which relevant features that uniquely characterize the objects in the images can be extracted. The extracted features then allow the computer to recognize similar objects in images that are not contained in the representative set. Techniques for feature extraction in image analysis commonly use a basis of functions to generate a subspace over which images are projected. The coefficients resulting from the projection are then, either directly or the result of a combination of them used as features to characterize the image. Many different types of invariant features and invariant representations have been studied (Brandt and Lin, 1996) (Lin and Brandt, 1993). An approach is to represent

About[1] -Yee Ming Chen, Department of Industrial Engineering and Management
Yuan Ze University, Taoyuan, Taiwan, Republic of China
About -[2]Jen-Hong Chiang, Department of Industrial Engineering and Management
Yuan Ze University, Taoyuan, Taiwan, Republic of China

the images with frequency domain invariants that are derived from the Fourier-Mellin transform. The magnitude of the Fourier-Mellin transform is invariant with respect to rotation and scaling, but is incomplete. Although several sets of rotation and scaling invariant descriptors have been designed under the Fourier-Mellin transform framework (Milanese and Cherbuliez, 1999), the incompleteness property could not usually be satisfied. This is because the phase spectrum was always ignored. In order to overcome this problem, Ghorbel in Ref. (Ghorbel, 1994) proposed a complete set of rotation and scaling invariants under the analytical Fourier-Mellin transform (AFMT) based on the complete complex spectra. All above invariant transform have been extensively used in Image Analysis since they allow the extraction of rotation and scale invariant features for image recognition. Wavelets are also popular families of functions to build basis sets for feature extraction (Sastry et al., 2004; Li et al., 2004). Because of their efficiency to identify temporal/spatial features in different types of data sets, wavelet functions have gained popularity in a large domain of data classification applications. In (Lee and Pun, 2003) a log-polar wavelet transform is used to extract rotation and scale invariant features for texture analysis. In (Shen and Ip, 1999) also proposes the extraction of shape descriptors using wavelet analysis.In this paper, a novel method of character identification based on the IC chips features extracted from the integrated discrete wavelet and the hybrid Fourier-AFMT framework (DWF-AFMT) is proposed. By using DWF-AFMT features, the distortion and alignment problems are alleviated while retaining the advantages of the image-based approach. In this proposed technique, discrete wavelet transform preserves the local edges and reduce the noise in the low frequency domain after the image decomposition, and hence makes the character images less sensitive to shape distortion. In addition to that, the reduced dimension of the images also helps to improve the computation efficiency. Fourier-AFMT produces a translation, rotation in plane and scale invariant feature. The linearity property of Fourier-AFMT enables multiple DWF-AFMT features to be used to form a reference invariant feature and hence reduce the variability of the input images. Based on the method, a IC chip character identification system has been designed.We exemplify the use of our framework using wavelet functions and measure the quality of the extracted IC chips features as image descriptors in an OCR experiment. The rest of this paper is organized as follows. In Section 2, we introduce the pattern recognition system which includes a DWF-AFMT framework. In Section 3, we report our experiments. Finally in the last section, we draw the conclusion and point out some directions for future research.

II. Pattern Recognition System

A pattern recognition system includes three modules, i.e. the preprocessing stage, the extracted IC chip feature stage and the classification stage.

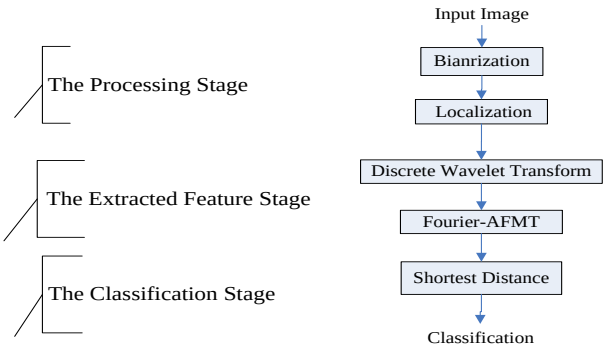

Figure 2. Block diagram of the proposed hybrid Fourier-AFMT and project profile combination framework

The framework of IC chip feature extraction is shown as Figure 2. Given an input face image, binarization converts the image pixels and the feature extractions are individually implemented with the hybrid Fourier-AFMT framework. Then classify an image feature by the shortest distance criterion.

A. The Processing Stage

The input image is initially processed to improve its quality by normalizing the image with some threshold which helps to offset the differences resulting form changing environmental and lighting conditions, etc. It increases the contrast for obtaining a suitable binary (black and white) image from the grey image obtained by camera for character identification. It involves

(1) Conversion of gray intensity image into a binary image by application of Canny method of segmentation (Canny, 1986). It finds edges by looking for local maxima of the gradient of the B & W image.

(2) Dilation using the linear morphological structuring element orthogonal to each other: Using this structuring element, holes and spots are filled, to make character localization easier.

(3) Sub-sampling: Averaging filter is applied, based on a fixed standard/threshold, in order to reduce the number of pixels herein in the image, leading to lesser computational complexity.

B. The Extracted Feature Stage

(1). Extract facial expression insensitive using wavelet transform

Wavelet transform is able to decompose image into a lower dimensional multi-resolution representation, which grants a compact hierarchical framework for interpreting the image information. The wavelet decomposition of a signal $f(x)$ can be obtained by convolution of signal with a family of real orthonormal basis, $\psi_{a,b}(x)$;

$$(W_\psi f(x))(a,b) = |a|^{-\frac{1}{2}} \int_{\Re} f(x)\psi\left(\frac{x-b}{a}\right)dx \qquad f(x) \in L^2(\Re) \quad (1)$$

where $a, b \in \Re, a \neq 0$ are the dilation parameter and the translation parameter respectively. The basis function

$\psi_{a,b}(x)$ is obtained through translation and dilation of a kernel function $\psi(x)$ known as mother wavelet as defined below:

$$\psi_{a,b}(x) = 2^{-a/2}\psi(2^{-a}x - b) \quad (2)$$

The mother wavelet $\psi(x)$ can be constructed from a scaling function, ψ(x). The scaling function ψ(x) satisfied the following two-scale difference equation

$$\phi(x) = \sqrt{2}\sum_n h(n)\phi(2x-n) \quad (3)$$

Where $h(n)$ is the impulse response of a discrete filter which has to meet several conditions for the set of basis wavelet functions to be orthonormal and unique. The scaling function ψ(x) is related to the mother wavelet $\psi(x)$ via

$$\psi(x) = \sqrt{2}\sum_n g(n)\phi(2x-n) \quad (4)$$

The coefficient of the filter $g(n)$ are conveniently extracted from filter $h(n)$ from the following relation

$$g(n) = (-1)^n h(1-n) \quad (5)$$

For 2D signal such as image, there exists an algorithm similar to the one-dimensional case for two dimensional wavelets and scaling functions obtained from one-dimensional ones by tensorial product. This kind of two-dimensional wavelet transform leads to a decomposition of approximation coefficients at level *j*-1 in four components: the approximations at level *j*, L_j and the details in three orientations (horizontal, vertical and diagonal), $D_{j\ vertical}$, $D_{j\ horizontal}$ and $D_{j\ diagonal}$:

$$L_j(m,n) = \lfloor H_x * \lfloor H_y * L_{j-1}\rfloor_{\downarrow 2,1}\rfloor_{\downarrow 2,1}(m,n) \quad (6)$$

$$D_{j\ vertical}(m,n) = [H_x * [G_y * L_{j-1}]_{\downarrow 2,1}]_{\downarrow 1,2}(m,n) \quad (7)$$

The original image is decomposed into four subband images. Similarly, we can obtain two levels of the wavelet decomposition by applying wavelet transform on the low-frequency band sequentially. According to wavelet theory, the low-frequency band is the smoothed version of original image with lower-dimensional space. It also contains the highest-energy content within the four subbands. The low-frequency band features are insensitive to_the expressions and small occlusion. Hence, if applying *n* level wavelet decomposition to the capital image, the recognition performance and space dimension were affected. In this paper, we let *n* = 2 applying in the letter images group.

(2). Analytical Fourier-Mellin transforms (AFMT)

This is then followed by our proposed hybrid complete invariant under the AFMT transform frameworks, respectively. For clarity, the basic notation used can be described as follows. We denote the Cartesian spatial domain by (*x*, *y*) and the Cartesian frequency domain by (*u*, *v*); we denote the log-polar coordinates by (*ρ*, *φ*) and the polar coordinates by (*r*, *θ*). When an image (or a spectra) is converted to the log-polar or polar coordinates, the intensity (or spectral) function name is preserved while the variable is replaced with (*ρ*, *φ*) or (*r*, *θ*), respectively.

(A). The analytical Fourier-Mellin transform

It is well known that the direct similarity group on the plane is equivalent to the space of polar coordinates:

$$\Pi = \{(r,\theta) | r > 0 and 0 < \theta < 2\pi\}$$

The Fourier-Mellin Transform on Π can be defined as:

$$\hat{f}(u,v) = M_f(u,v) = \int_0^{+\infty}\int_0^{2\pi} f(r,\theta)e^{-iu\theta}r^{-iv}\frac{dr}{r}d\theta, \quad (8)$$

for $u \in Z$ and $v \in R$

It is the Fourier-Mellin Transform of the irradiance distribution *f(r, θ)* in a two-dimensional image expressed in polar coordinates can be taken in the image center of gravity in order to obtain invariance under translations.

The integral (8) diverges in general, since the convergence is indeed under the assumption that *f(r, θ)* is equivalent to Kr^{α} (α>0 and K a constant) in a neighborhood of the origin (the center of gravity of the observed image). For this reason, the Analytical Fourier-Mellin transform (AFMT) was defined by

$$M_f(u, s=\sigma+iv) = \int_{R^+}\int_0^{2\pi} f(r,\theta)e^{-iu\theta}r^{\sigma+iv}\frac{dr}{r}d\theta, \quad (9)$$

For $u \in Z$, $v \in R$ and $\sigma > 0$. f is assumed to be square summable under the measure dθdr /r.

The AFMT of an object *f* can be seen as the usual FMT of the distorted object $f_\sigma(r,\theta)=r^\sigma f(r,\theta)$. The AFMT gives a complete description of gray-level objects since *f* can be retrieved by its inverse transform given by

$$f(r,\theta) = \int_R \sum_{v\in Z} M_f(u,\sigma+iv)e^{iu\theta}r^{\sigma+iv}dv$$

With a variable change on the integral (q=ln(*r*) instead of *r*), the equation (9) can be rewritten into Fourier transforms as follows:

$$M_{f_\sigma}(u,v) = \frac{1}{2\pi}\int_{-\infty}^{+\infty}\int_0^{2\pi} e^{q\sigma}f(e^q,\theta)e^{-i(u\theta+qv)}d\theta dq \quad (10)$$

A fast algorithm is obtained by computing a two dimensional Fast Fourier Transform on the log-polar distorted object $e^{q\sigma}f(e^q,\theta)$.The log-polar sampling is built from the points obtained by the intersection between N beans originating from the image centroid and M concentric circles with exponentially increasing radii. In this paper, we have chosen N=80 and M=80 for E, F, H and T Database, and σ= 0.5 (Fig.3)

Fig.3 The original image (left), The log-polar image of origin (middle), the magnitude image of AFMT (right).

Let us recall the transformation law of the analytical Fourier-Mellin transform for planar similarities. Let g be the

orientation and size change of an object f by the angle $\beta \in [0;2\pi]$ and the scale factor R_+^*, i.e. $g(r,\theta) = f(\alpha r, \theta + \beta)$. These two objects have the same shape and denoted similar objects. One can easily shows that the AFMT of g and f are related by :

$$M_{g_\sigma}(k,v) = \alpha^{-\sigma+iv} e^{ik\beta} M_{f_\sigma}(k,v) \quad (11)$$

For all *k* in Z, *v* in R and σ>0.

Equation (11) is called the shift theorem and suggests that the AFMT is well suited for the computation of global shape features which are invariant to the object position, orientation and size.

(B). A complete set of Fourier-Mellin features

Since the usual Fourier-Mellin transforms of two similar objects only differ by a phase factor (Eq. (11) without the $\alpha^{-\sigma}$ term), a set of global invariant descriptors regardless of the object position, orientation and size, is generally extracted by computing the modulus of some Fourier-Mellin coefficients (Crimmins, 1982). A set like this is not complete since the phase information is lost and it only represents a signature of the shape. Due to the lack of completeness, one can find distinct objects with identical descriptor values and a classification process may mix up objects, which is critical for content-based retrieval from image database (both false positive and true negative matches).

Recently, a complete family of similarity invariant descriptors based on the AFMT has been suggested (Ghorbel, 1994). This family can be easily written and applied to any strictly positive σ value as follows:

$$I_{f_\sigma}(k,v) = M_{f_\sigma}(0,0)^{-\sigma+iv} \cdot e^{ikArg(M_{f_\sigma}(1,0))} \cdot M_{f_\sigma}(k,v) \quad (12)$$

for all *k* in Z , *v* in R.

Each feature *I*(*k*, *v*) is constructed in order to compensate the $\alpha^{-\sigma+iv} e^{ik\beta}$ term that appears in the shift theorem (11). The compensation is achieved via the two Fourier-Mellin coefficients, M(0, 0) and M(1, 0), which are the normalization parameters. The set in Eq. (12) is complete since it is possible (i) to recover the FMT of an object from all of their invariant descriptors and the two normalization parameters by inverting Eq. (12); (ii) to reconstruct the original image by the inverse AFMT.

C. Proposed Fourier-AFMT transforms

When considering the translation, rotation and scaling together, we combine the translational invariant with the rotation and scaling invariant to construct a hybrid complete invariant under the Fourier-Mellin transform scheme. Indeed the translation property of the Fourier transform is the basis of these above invariants, which is also satisfied in the complex domain. Through the combination of Fourier invariant and AFMT invariant, we can construct a hybrid complete similarity invariant as followings:

$$S(\cdot) = AFMT(F(\cdot)), \quad (13)$$

Note that because AFMT(.) is directly applied to a complex spectrum but not separately applied to a magnitude spectrum and a phase spectrum to generate two invariant descriptors, the obtained hybrid invariant descriptor is complete.

But then, due to the reciprocal scaling property of the Fourier transform, when the property of Eq. (11) is applied in the polar domain of Fourier spectra, it needs to be modified as follows:

$$M_{g_\sigma}(k,v) = \alpha^{\sigma-2-ik} e^{iv\beta} M_{f_\sigma}(k,v) \quad (14)$$

The AFMT invariant of Eq. (12) is also modified as follows:

$$I_{f_\sigma}(k,v) = \left|M_{f_\sigma}(0,0)\right|^{(-\sigma+2+ik)/(\sigma-2)} \cdot \exp(-i \operatorname{var} g(M_{f_\sigma}(0,1))) \cdot M_{f_\sigma}(k,v) \quad (15)$$

In the same manner as Eq. (13), we can construct a hybrid complete invariant under the AFMT scheme as follows:

$$S(\cdot) = AFMT_M(F(\cdot)) \quad (16)$$

III. Classification Stage

For IC chips features recognition purposes, the classification of an unknown object into a set of reference patterns is achieved by several comparison methods. Besides them, the direct comparison of a couple of features, neural networks, or statistical classifiers, by means of intra- and inter-class similarity measures.

Since the invariant set of Eq.(12) is also convergent for square summable functions, it can be shown that the following function defines a true mathematical distance between shapes (Ghorbel, 1994):

$$d_2(I_{f_\sigma}, I_{g_\sigma}) = \left[\int_{-1}^{+1} \sum_{k \in z} \left|I_{f_\sigma}(k,v) - I_{g_\sigma}(k,v)\right|^2 dv\right]^{1/2} \quad (17)$$

This distance is an Euclidean distance expressed in the invariant domain. Theoretically, it is zero if and only if the objects are identical up to a similarity transformation. Due to numerical sampling and approximation, we never have exactly zero and the value of the distance is used for the quantification for the similarity between objects, regardless of their pose, orientation and size in the image.

IV. Experiments and Results

Four binary images were used as IC chip feature prototypes, each containing a capital letter E, F, H, or T. Each letter has a uniform intensity equal to 1, and the uniform background of the images is set to 0. From each prototype, 96 versions are obtained by scale, orientation, or noisy changes of the letter (Fig.4). The resultant images show that the original feature image is low in contrast and has low gray levels. The 96 images containing the same letter are considered an image group. The invariant features M_{f_σ} for each image in the group should be identical.

Because translation will not change the relative position of the centre of mass of the letter, our major concern is the AOI system's performance on rotation angles are 30, 60, 90, 120, 180 and 240^0, and the four different scaling factors are 0.6, 0.8, 1.0 and 1.2. The noisy images are added at three levels with Gaussian noise having a mean value equal to 0 and a standard deviation(SD) equal to 0.04, 0.08 and 0.12. In this paper, 2 levels decomposition are performed on a image

with size 300 × 300 pixels. The 80 × 80 pixels sub-images have been chosen and it was interpolated and re-sampled in log-polar coordinates with 80 beans in the angular direction and 80 concentric circles in the radial direction.

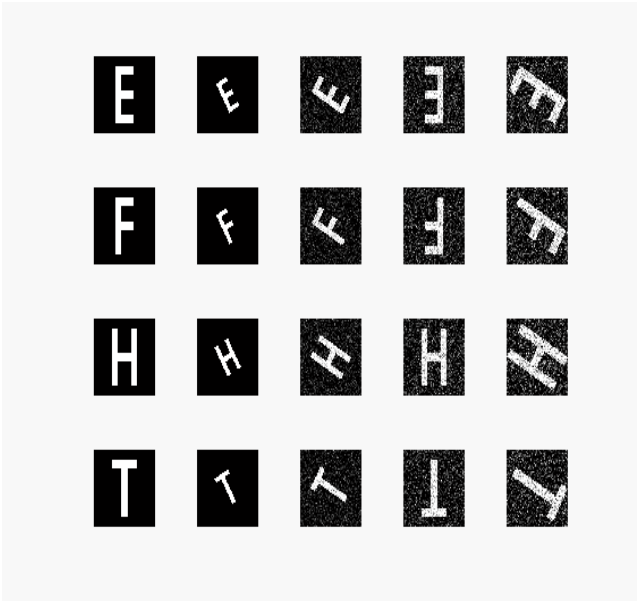

(1) (2) (3) (4) (5)

Fig. 4. parts of four pattern groups: (1) with prototypes; (2) scaled by the factor 0.6 and with rotated by 30^0; (3) scaled by the factor 0.8, rotated by 60^0 and with noise SD 0.04; (4) with prototype, rotated by 180^0, and with noise SD 0.08; (5)

In the proposed method, Fourier-AFMT is based on Fourier Transform theory, which has a linear property. This implies that multiple m DWF-AFMT features can be used to form a reference DWF-AFMT feature and just only one representation per user needs to be stored in the database. The representation for each user, ($DWF\text{-}AFMT_{ui}$) can be formulated as follow:

$$DWF \cdot AFMT_{ui} = \frac{1}{m}\sum_{j=1}^{m} DWF \cdot AFMT_j^i$$

Where DWF-AFMT, is the invariance feature of the j^{th} view image of the i^{th} character. Producing a $DWF\text{-}AFMT_u$ feature from different training images, could relax various variability that occur during the acquisition process, such as sharp distortion and noise.

A. Classification in feature space

A database of 384 images of size 300×300 including 96 images per character from 4 characters have been used for experiments. We have chosen 80×80 sub-images such that the central sub-image to be entirely located in the pattern in all images. Each image is thus represented in a 441 dimensional feature space obtained by the magnitude of central analytical Fourier-Mellin harmonics (K=V=10). The recognition performances achieved by using the proposed DWF-AFMT features have been evaluated using a k-NN classifier. A number of k images from each character (for a total of 4k images) have been used as the training set, whereas the remaining 96-k images from each character (for a total of 4× (96-k)) have been used for testing. The interclass distances among the four prototypes are given in Table 1. The intraclass distances for each group of pattern points is defined by the mean-square error

$$\sigma = \frac{1}{N-1}\sum_{i=2}^{N}\left\|(M_f)_i - (M_f)_1\right\|^2,$$

Where N = 24 is the total number of images in the group and i=1 corresponds to the prototype. The root-mean-square errors for each group are given in Table 2, which are taken as clustering criteria for the images groups. By comparison with the interclass distances in Table 1, all four image groups are well clustered and well separated from one another.

Table 1. Interclass Distances among prototypes E, F, H

prototypes	E	F	H	T
E	0	0.4676	1.3515	0.7939
F	0.4676	0	1.3046	0.7674
H	1.3515	1.3046	0	1.5798
T	0.7939	0.7674	1.5798	0

Table 2. Intraclass Distances for the Image Groups E, F, H and T

prototype	E	F	H	T
σ	0.8683	0.7968	1.1424	0.5943

By comparison with the interclass distances of Table 1 and 2, an explanation for this may be as follows. The first one is that the interclass distance between capital letter E and F tend to be smaller than that between capital letter E and H. When interclass distance between two characters is small, any variation on digit will lead this digit to be easily confused with the other. The second reason why capital letter E and F digits are harder to classify than H and T digits is that the variance in image groups H and T are in general higher than that in case of E and F. The comparison characters images recognitions are done by studying the performances of different classification techniques. Five different nearest neighbor rule from k = 1 to k = 5, table 3 shows the results for higher nearest neighborhood classifiers of better recognition rate comparison.

Table 3. Comparison of 5 classification techniques on characters images recognitions

K-NN	1-NN	2-NN	3-NN	4-NN	5-NN
Recognition rate	0.73	0.92	0.92	0.96	0.97

The recognition rate from each noisy (SD=0.04, 0.08 and 0.12) and deformed image to all the four prototypes are shown in Table 4. By the nearest neighbor rule, these noisy images recognition rate showed in a descending order form top to bottom. It is clear that the decay of recognition rate of different classifiers for all the cases.

Table 4. Comparison of 5 classification techniques on characters noisy images recognitions

Recognition rate	SD=0	SD=0.04	SD=0.08	SD=0.12
1-NN	0.73	0.60	0.53	0.41
2-NN	0.92	0.72	0.52	0.5
3-NN	0.92	0.67	0.45	0.35
4-NN	0.96	0.64	0.44	0.32
5-NN	0.97	0.66	0.46	0.33

The recognition performances achieved by using the proposed DWF-AFMT features have been evaluated using different (K,V) pairs. The most interesting observation may be noticed from Table 5. It increases almost linearly with (K,V) pairs for different noise conditions. This result shows that, in general, that higher value (K,V) are more robust against noise.

Table 4. Comparison of different (K,V) of the proposed DWF-AFMT on characters noisy images recognitions

Recognition rate	SD=0	SD=0.04	SD=0.08	SD=0.12
K=V=7	0.97	0.65	0.41	0.30
K=V=10	0.97	0.66	0.46	0.32
K=V=15	0.97	0.72	0.54	0.43
K=V=20	0.97	0.73	0.55	0.46

B. Recognition results

We use 5 - NN classifier, have 3 misclassifies only. As the following experiment, 75% recognition rate for a misclassified. The recognition results for different scaling factors are given in Table 5, while the recognition results for a combination of rotation and scaling are shown in Table 6. We shall emphasis on testing for robustness to noise in Table 7. These results demonstrate the effectiveness of this feature extraction algorithm against geometric variation.

Table 5. Recognition result for different scaling factors

Scale factors	0.6	0.8	1.0	1.2
Recognition rate	75%	100%	100%	100%

Table 6. Recognition rate for different rotation angles and scaling factors

	30^0	60^0	90^0	180^0	240^0
0.6	100%	100%	100%	75%	100%
0.8	100%	100%	100%	100%	100%
1.2	100%	100%	75%	100%	100%

V. Conclusion

In this paper, we proposed the integrated discrete wavelet and the hybrid Fourier-AFMT framework (DWF-AFMT) for IC chips marking inspection. We focus our attention in this contribution on two particular points. The first one deals with the computation of a new set of invariant features allowing the classification of multi-oriented and multi-scaled patterns the estimation of characters orientation. From this point, the interests of this computation rely on the possibility to use this Analytical Fourier Mellin transform within a "filtering mode" that permits to solve the difficult problem of optical character recognition. The second point deals with the characters noisy images. These results are in agreement with the analysis of Section 3.1. They confirm that DWF-AFMT is more robust against noise. In this paper, we also present four different feature extraction methods have been studied for the marking inspection. The recognition accuracy of the proposed methods with 5-NN classifier is over 97%. As a conclusion, the proposed system is successfully developed and tested to solve the semiconductor industry problems

Acknowledgements

This research work was sponsored by the National Science Council, R.O.C., under project number NSC98-2221-E-155-023.

VI. References

1) Cho, C. S, Chung, B.M. and Park, M.J., (2005) Development of real-time vision-based fabric inspection system, IEEE Trans Industrial Electron, 52 , Pp.1073-1079.
2) Mantas, J.(1986) An Overview of Character Recognition Methodologies", Pattern Recognition, V0119(6), Pp.425-430.
3) Shunji Mori, Ching Y. Suen and Kazuhiko Yamamoto (1992) Historical Review of OCR Research and Development", Proceedings of the IEEE, vol80 (7), Pp. 185-201.
4) Adnan Amin, Humoud Al-Sadoun and Stephen Fischer (1996) Hand-Printed Arabic Character Recognition System Using An Neural Network", Pattern recognition, vol.29(4), Pp. 663-675.
5) Nagarajan, R., Sazali Yaacob, Paulraj Pandian, Karthigayan, M. Shamsudin Hj Amin and Marzuki Khalid (2003) A Neural Network Application for Inspecting the Marking of Symbols on Integrated

Circuit Chips". The 7th Triennial AEESEAP Conference Enhancing Engineering Education and Training, Malaysia, 8-9 August 2003,Pp. 1145-1161.

6) Pan, Wumo , Jin, Jianming, Shi, Guangshun and Wang, Q.R. (2001) A System for Automatic Chinese Business Card Recognition. Proceedings of the Sixth International on Document Analysis and recognition", IEEE Computer society, Pp. 577 – 581.
7) Gonzalez, Rafael C. and Woods, Richard E.(1993) Digital Image processing, Addison-Wesley Longman, Inc..
8) Mauritius, Seeger and Christopher, Dance. (2001). Binarising Camera Images for OCR. Proceedings of Sixth International Conference on Document Analysis and Recognition, 54 – 58.
9) Oivind, Due Trier , Anil, K.Jain and Torfinn, Taxt, (1996) Feature Extraction Methods for Character Recognition a Survey", Pattern Recognition, Vol.29(4), 641-662.
10) Brandt , R. D., Lin, Feng (1996) Representations that uniquely characterize images modulo translation, rotation and scaling", Pattern Recognition letters 17, Pp.1001-1015.
11) Lin, F. and R. D. Brandt. (1993) "Towards absolute invariants of images with respect to translation, rotation and scaling". Pattern Recognition letters 14 (5), Pp. 369-379.
12) Milanese , R., Cherbuliez , M., (1999) A rotation, translation, and scale invariant approach to content-based image retrieval, J. Visual Commun. Image Representation 10, Pp. 186-196.
13) Ghorbel, F. (1994) A complete invariant description for gray-level images by the harmonic analysis approach, Pattern Recognition Lett. 15, Pp. 1043-1051.
14) Sastry, C. S., Pujari, A. K., Deekshatulu, B. L., and Bhagvati C.(2004) A wavelet based multiresolution algorithm for rotation invariant feature extraction", Pattern Recognition Letters, Vol. 25, Pp. 1845-1855.
15) Li, C., Huang, J-Y., Chen, C-M.(2004) Soft computing approach to feature extraction", Fuzzy sets and systems, Vol. 147, Pp. 119-140.
16) Lee, M..C., and Pun, C.M.(2003) Rotation and Scale Invariant Wavelet Feature for Content-Based Texture Image Retrieval", Journal of the America Society: for Information Science and Technology, Vol 54. No. 1, Pp. 68-80.
17) Shen, D. and Ip H.(1999) Discriminative wavelet shape descriptors for recognition of 2D patterns", Pattern Recognition, Vol 32, Pp.. 151-165.
18) Canny, J (1986) A Computational Approach to Edge Detection", IEEE Transactions on Pattern Analysis and Machine Intelligence, vol. 8, Pp. 679-698.
19) Crimmins,T.R.(1982) A complete set of Fourier descriptors for two dimensional shapes", IEEE Trans. Syst., Man, Cybern. 12(6), Pp. 848-855.
20) Ghorbel, F.(1994) A complete invariant description for grey-level images by the harmonic analysis approach", Pattern Recognition Lett. 15, Pp. 1043-1051.